Molecular Therapy
Oncolytics
Original Article

A PD1 targeted nano-delivery system based on epigenetic alterations of T cell responses in the treatment of gastric cancer

Nan Hu,[1,4] Wei Li,[2,4] Yidong Hong,[1,4] Zengtao Zeng,[3] Jingzhou Zhang,[1] Xueyu Wu,[1] Kangjie Zhou,[1] and Fenglei Wu[1]

[1]Department of Oncology, The First Affiliated Hospital of Kangda College of Nanjing Medical University, The First People's Hospital of Lianyungang, Lianyungang, Jiangsu 222000, China; [2]Center of Research Laboratory, The First Affiliated Hospital of Kangda College of Nanjing Medical University, The First People's Hospital of Lianyungang, Lianyungang, Jiangsu 222000, China; [3]Department of General Surgery, The First Affiliated Hospital of Kangda College of Nanjing Medical University, The First People's Hospital of Lianyungang, Lianyungang, Jiangsu 222000, China

The anticancer effects of immune checkpoint inhibitors (ICIs) have been widely examined recently. Although ICIs have been progressively improved for successful gastric cancer treatment, different trials of ICIs such as pembrolizumab and nivolumab have yielded widely variable response rates. Strategies to further improve the efficacy of ICIs are still needed. Previous studies have shown that *de novo* DNA methylation is acquired by PD1+CD8+ tumor-infiltrating T cells (TILs), which cause a hierarchical downregulation of cytokines such as interferon-γ (IFN-γ). The epigenetic agent 5-Aza-2′-deoxycytidine (DAC) blocks *de novo* DNA methylation in activated PD1+CD8+ TILs. Such a feature might help enhance the anti-tumor effect of immune checkpoint blockade (ICB) treatment. In this study, polyethylene glycol-poly(ε-caprolactone) (PEG-PCL) nanoparticles (NPs) were linked to the anti-programmed death-1 monoclonal antibody nivolumab to yield αPD1-NPs for targeting TILs with PD1 overexpression using DAC. In addition, the NPs increased DAC stability and improved IFN-γ secretion and the anti-tumor effect of ICB *in vitro*. Therefore, targeted delivery of DAC reverses the exhaustion of PD1+CD8+ TILs and improves T cell responses and the treatment effect of ICB. These findings suggest that nivolumab-NPs are a potential tool for the delivery of epigenetic drugs, which could enhance the anti-tumor effect of ICB in gastric cancer.

INTRODUCTION

Gastric cancer (GC) is a common malignancy in China, with about 400,000 new cases reported each year.[1] Most individuals with GC are diagnosed at an advanced stage and are not eligible for surgery. Despite significant progress in radiotherapeutic and chemotherapeutic treatments, prognosis in advanced gastric cancer remains poor, and treatment options are limited.

Tumor immunity is divided into cellular and humoral immunity. Cellular immunity is the main component; specifically, tumor-infiltrating lymphocytes (TILs) mediating cellular immunity are the main force against tumors. During the tumor immunization process, antigen-presenting cells take up and process the tumor antigen and present the processed antigen to T lymphocytes to induce an anti-tumor immune response. Most human tumors have abnormal expression of oncogenes or tumor suppressor genes specific to tumor cells, and their products can be recognized by T cells, which have become a hotspot in tumor immunotherapy research.[2] A recent study examining the effector IFN-γ and exhaustion phases of immune responses revealed gradually acquired heritable *de novo* methylation programs suppressing T cell expansion and clonal diversity in the course of PD1 blockade therapy.[3] The immunity induced by this tumor-associated antigen gradually enters the "exhaustion" phase because of the expression of the immunoregulatory factor programmed death receptor 1 (PD1).[4] Therefore, blocking the PD1/PDL1 pathway by anti-PD1 antibody (αPD1) or anti-PD1 ligand 1 (αPDL1) can potentially revert T cell exhaustion and enhance anti-tumor immune responses in individuals with various advanced malignancies, including melanoma and lung, liver, and gastric cancers. These exhaustion-related DNA methylation programs were acquired in PD1+CD8+ TILs, and application of DNA methyltransferase suppressors, including 5-Aza-2′-deoxycytidine (DAC), reversed these programs, sensitizing tumors to PD1/PDL1 checkpoint blockade therapy.[3] Another study showed that single-agent DAC leads to increased CD8+ tumor-infiltrating T cells and PD1 expression. Although immune checkpoint inhibitors (ICIs) alone had modest effects, DAC combined with ICI therapy additively suppressed tumor cell proliferation and increased the survival time of pancreatic ductal adenocarcinoma-bearing mice.[5]

DAC is the most broadly assessed demethylating drug.[6] It has been approved for myelodysplastic syndrome (MDS) and exerts anti-leukemic effects in acute myeloid leukemia (AML).[7] Its effects on solid tumors are currently being investigated. Drug instability

Received 5 August 2021; accepted 7 December 2021;
https://doi.org/10.1016/j.omto.2021.12.006.

[4]These authors contributed equally

Correspondence: Fenglei Wu, Department of Oncology, The First Affiliated Hospital of Kangda College of Nanjing Medical University, The First People's Hospital of Lianyungang, Lianyungang, Jiangsu 222000, China.
E-mail: wufenglei1981@163.com

constitutes the main drawback of DAC in cultured cells (half-life 17 h,[8] aqueous solution [12 h])[9] and animal models.[10] Therefore, its efficacy in solid tumors is limited.[9]

Nivolumab, a fully humanized immunoglobulin G4 monoclonal antibody (mAb), interacts with the PD1 membrane receptor.[11] The ATTRACTION-2 (ClinicalTrials.gov identifier NCT02267343) study, on the basis of which nivolumab was approved in Japan, Korea, Taiwan, and Switzerland for cases of unresectable advanced or recurrent GC after progression following chemotherapy, revealed that nivolumab demonstrates superior overall survival (OS) over placebo (median OS 5.3 vs 4.1 months).[12] Unfortunately, despite the considerable success of that study, only a subset of affected individuals benefited from nivolumab (overall response rate [ORR] 11.9%).[12] Moreover, a subset of affected individuals experience progression again after clinical remission.[6] Hence, it is an urgent need to increase the efficacy of immune checkpoint blockade (ICB) treatment in GC.

For decades, nanoparticle (NP)-based drug delivery systems have markedly transformed the field of cancer therapy. NPs possess multiple advantages compared with traditional delivery techniques, such as an enhanced permeation and retention (EPR) effect via leaky tumor vessels and active targeting mechanisms, with NPs functionalized with specific ligands or antibodies interacting with receptors on targeted cells. Novel paradigms using nanomedicine for immune cell engagement are emerging. Such nanomedicines activate cytotoxic anticancer T cell responses instead of merely delivering drugs to the tumor.[13] According to a recent study in which we prepared trastuzumab-NPs-DAC to prolong the degradation time of DAC,[14] we conjugated αPD1 (i.e., nivolumab) with poly(ethylene glycol) (PEG) and poly(ε-caprolactone) (PCL) copolymers, with PEG as the linker (αPD1-PEG-PCL). DAC was encapsulated in αPD1-PEG-PCL by the double-emulsion solvent evaporation method. Receptor-mediated CD8+ TIL targeting was achieved via PD1 overexpression. In this study, we hypothesized that αPD1 can be used not only to target nanoparticles to given cells but also to convey immune checkpoint blockade, thus further reversing T cell exhaustion. We further hypothesized that prolonged DAC half-life and efficient intracellular delivery sustain re-secretion of the effector IFN-γ to enhance response to ICB therapy.

Therefore, in this study we examined whether the particles could be targeted to PD1+CD8+ TILs. Interestingly, the particles were indeed targeted to functional markers (e.g., PD1). In addition, targeted delivery of DAC to PD1-expressing TILs more pronouncedly inhibited autologous tumor cells compared with the free drug. These data indicate DAC delivery with PD1-NPs may be a potential therapeutic tool in GC.

RESULTS

Preparation of αPD1-PEG-PCL copolymer

αPD1-PEG-PCL copolymers were synthesized as described in Materials and methods. Carboxyl groups on antibody molecules were activated and reacted with primary amino groups on PEG-PCL polymers, linking antibody molecules on NPs. X-ray photoelectron spectroscopy (XPS) was performed to detect changes in nitrogen signals on the basis of specific binding energy, to confirm the conjugation. Nivolumab, with 1,714 nitrogen atoms, showed signals with higher intensity compared with the amino groups of PEG-PCL polymers. Different peaks from nitrogen (N 1s) indicated antibody linking in the polymer's core, although non-linked NPs also presented weaker signals reflecting nitrogen atoms in surface amino groups. Therefore, antibodies were successfully conjugated with the polymer's matrix (Figure 1A).

Ligand surface density

The association of antibody conjugates on NPs with the PEG-PCL/nivolumab ratio was examined. Multiple levels (w/w) of PEG-PCL/nivolumab (20%, 40%, 60%, and 80%, respectively) were used for αPD1-PEG-PCL copolymer preparation. The final concentrations of nivolumab linked to NPs' surface were 0.095, 0.185, 0.228, and 0.219 mg/mg NPs following background (no NPs) subtraction, respectively (Table 1). Therefore, 60% was selected as the PEG-PCL/nivolumab ratio for αPD1-PEG-PCL copolymer synthesis in further assays.

Preparation and characterization of DAC-loaded NPs

NPs-DAC and αPD1-NPs-DAC syntheses were carried out as described above. NPs without drugs constituted the controls. The produced NPs were 185.3–223.6 nm, facilitating their enrichment in tumors by EPR enhancement.[15] Zeta potential values were negative, between −8.16 and −10.93 mV; polydispersity ranged between 0.179 and 0.301 (Table 2). Transmission electron microscopy (TEM) (Figure 1B) showed that αPD1-NPs-DAC were spherical, with diameters approximating 200 nm on average. The DLCs of DAC in NPs-DAC and αPD1-NPs-DAC were 8.11% ± 0.12% and 8.21% ± 0.18%, respectively. The encapsulation efficiencies (EEs) of DAC in NPs-DAC and αPD1-NPs-DAC were 57.32% ± 2.3% and 59.2% ± 3.2%, respectively. The nivolumab contents of αPD1-NPs and αPD1-NPs-DAC were 3.84% ± 0.23% and 3.62% ± 0.19%, respectively (Table 2). This αPD1-NPs-DAC formulation provided a nivolumab-to-DAC mass ratio of 1:2.26.

Structural stability and DAC degradation assay for αPD1-NPs-DAC in PBS

The particle sizes of αPD1-NPs-DAC and NPs-DAC were stable beyond 2 weeks (Figure 1C). Serum stability was used to determine the abilities of αPD1-NPs and NPs to protect DAC. Here, free DAC, PEG-PCL-DAC, and αPD1-PEG-PCL-DAC underwent incubation with fetal bovine serum (FBS) at 37°C for various times. PEG-PCL and αPD1-PEG-PCL NPs prevented DAC degradation for up to 72 h (Figure 1D). Meanwhile, free DAC was decomposed within 12 h. These findings indicated that DAC's half-life could be markedly increased after encapsulation in PEG-PCL and αPD1-PEG-PCL NPs.

Cellular uptake

αPD1-NPs and NPs were stained with 1,1-dioctadecyl-3,3,3,3-tetramethylindodicarbocyanine (DiD). As shown in Figure 2, red fluorescent

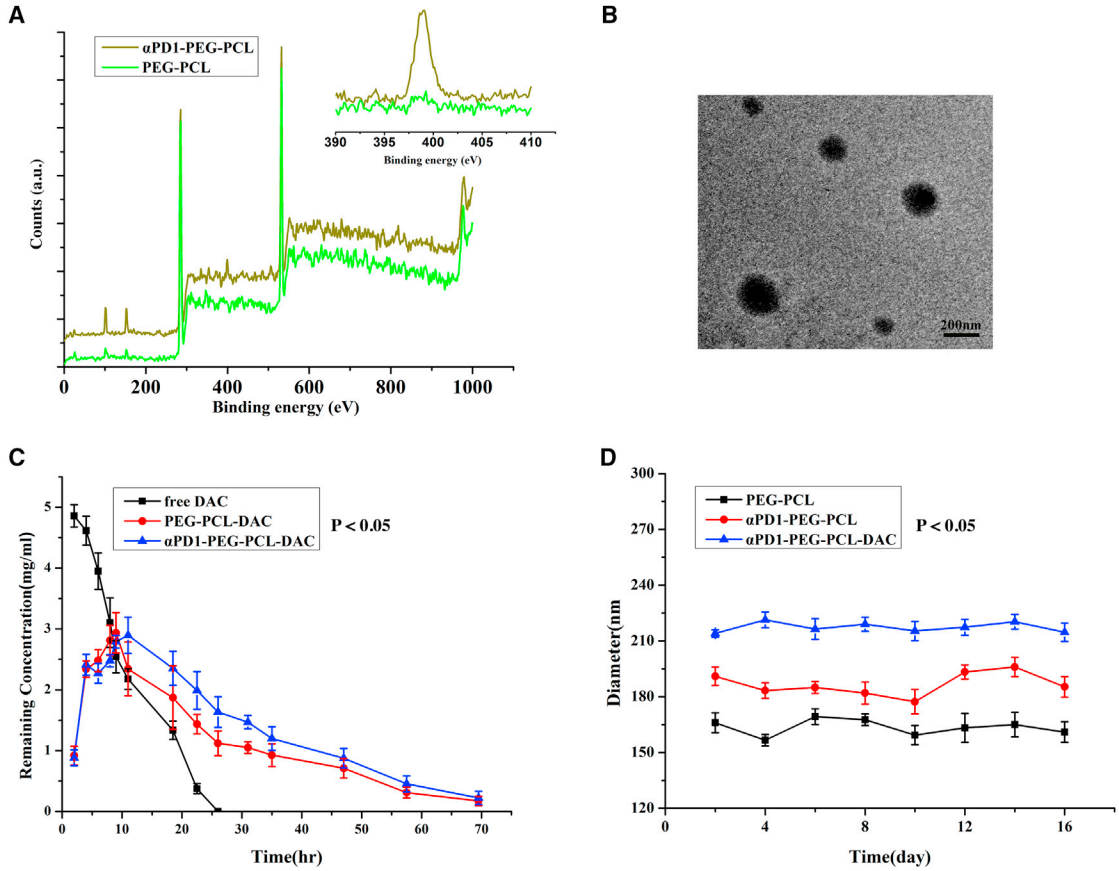

Figure 1. Characterization of αPD1-PEG-PCL-DAC

(A) Representative XPS spectrum and N 1s peak (inset) of the αPD1-PEG-PCL nanoparticles before (lower curve) and after (upper curve) nivolumab conjugation. (B) Morphology of αPD1-PEG-PCL-DAC by TEM. Scale bar represents 200 nm. (C) Stability study of NPs. The diameters of NPs were determined using DLS, and data are presented as mean ± SD. (D) Change in DAC remnant in the following groups: free DAC, NPs-DAC, and αPD1-NPs-DAC in PBS. Data are presented as mean ± SD. XPS, X-ray photoelectron spectroscopy; TEM, transmission electron microscopy; NPs, nanoparticles; DLS, dynamic light scattering.

signals from DiD-labeled nanoparticles were found in the cytoplasm, indicating that αPD1-NPs and NPs entered into the cytosol. PD1+CD8+ TILs were used as a positive control to compare TILs with no PD1 expression. In PD1−CD8+ TILs, the integrated optical densities (IODs) of DiD showed no significant difference between the PEG-PCL and αPD1-PEG-PCL groups ($p > 0.05$) (Figures 2A and 2B; Table 3). However, the IOD of DiD was markedly elevated in the αPD1-PEG-PCL group compared with the PEG-PCL group in PD1+ TILs ($p < 0.001$) (Figures 2C and 2D; Table 3). The IODs of DiD in the PEG-PCL group suggested comparable cellular uptake levels in PD1+CD8+ TILs and PD1−CD8+ TILs ($p > 0.05$) (Figures 2B and 2D; Table 3), while the αPD1-PEG-PCL group exhibited higher cellular uptake in PD1+CD8+ TILs ($p < 0.001$) (Figures 2A and 2C; Table 3), indicating that αPD1-PEG-PCL nanoparticles were effectively targeted into PD1+CD8+ TILs.

Inhibitory effect on the growth of co-cultured cells

We used PD1+CD8+ TILs (Figure 3A) or autologous tumor cells to assess the cytotoxic abilities of saline (saline control), empty NPs, free DAC (12 μmol/L), free nivolumab (1 μg/L), free DAC + free nivolumab, blank αPD1-NPs (equal nivolumab levels), NPs-DAC (equal DAC concentration), NPs-DAC+αPD1, and αPD1-TNPs-DAC (equal concentrations of DAC and nivolumab) using the MTT assay. We found that cells administered blank NPs showed maximal cell viability. DAC (free or NP encapsulated) showed only a limited impact on cell viability for 4 days, indicating no overt cytotoxicity (Figures 3A–3C). Autologous tumor cells co-cultured with PD1+CD8+ TILs administered αPD1-NPs had comparable cytotoxicity as nivolumab. These cells had higher cell death levels when administered αPD1-NPs-DAC compared with free nivolumab, DAC + nivolumab, and NPs-DAC + nivolumab. Besides, the longer the time, the greater the difference in the cytotoxicity of αPD1-NPs-DAC compared with other experimental groups (Figures 3A, 3D and 3E).

αPD1-NPs-DAC enhance mortality of tumor cells

The co-culture system, applying CFDA-SE-stained autologous tumor cells and subtype TILs from individuals with GC, was used to

Table 1. Nivolumab content of the nivolumab-PEG-PCL nanoparticles of various PEG-PCL amounts used in the nanoprecipitation process

Ratio of PEG-PCL to Nivolumab, % w/w	Nivolumab Content, % w/w[a]
20	2.5 ± 0.11
40	3.6 ± 0.08
60	3.8 ± 0.06
80	3.7 ± 0.09

[a]The SD value is for the mean trastuzumab content (% w/w) obtained from three measurements.

investigate the anticancer activity of immunotherapy. After treatment with saline, empty NPs, free DAC, free nivolumab, free DAC + free nivolumab, αPD1-NPs, NPs-DAC, and αPD1-NPs-DAC for 72 h, the death of autologous tumor cells was assessed using flow cytometry. As depicted in Figure 4, the saline control group had slightly higher cytotoxicity (3.9% ± 0.4%) in comparison with spontaneous death in autologous tumor cells (1.8% ± 0.1%), suggesting that PD1+CD8+ cells derived from individuals with GC had slight cytotoxicity against autologous tumor cells. Besides, a larger number of apoptotic tumor cells was observed in the αPD1-NPs-DAC group (44.11% ± 3.4%) in comparison with cells administered saline control (3.9% ± 0.4%), empty NPs (4.82% ± 2.14%), DAC (6.13% ± 3.12%), αPD1 (22.01% ± 3.5%), αPD1-NPs (25.13% ± 2.22%), DAC-NPs (8.39% ± 2.31%), or NPs-DAC+αPD1 (29.11% ± 3.5%) ($p < 0.01$; Figure 4).

Cytokine levels

TILs release cytokines such as IFN-γ, activating immune responses to inhibit virus-infected and cancer cells. As αPD1-NPs-DAC increased the anti-tumor effects of PD1+CD8+ TILs, we next assessed whether αPD1-NPs-DAC enhances cytokine secretion in PD1+CD8+ TILs after 24, 48, and 72 h of treatment. ELISA showed that in comparison with the blank NP control group, free DAC (12 μmol/L), nivolumab (1 μg/L), NPs-DAC (equal to DAC amounts), and αPD1-NPs-DAC (equal to DAC and nivolumab concentrations) could all increase the secretion level of IFN-γ after treatment for 48 h, by 1.33-fold ($p > 0.05$), 2.23-fold ($p < 0.01$), and 3.06-fold ($p < 0.01$), respectively (Figure 5A). Notably, the difference in IFN-γ secretion in the αPD1-NPs-DAC group was more obvious at 72 h (4.16-fold), whereas the NPs-DAC group almost kept its level at 48 h (Figure 5A). This result clearly showed that αPD1-NPs-DAC could increase IFN-γ production in PD1+ TILs. In PD1−CD8+ TILs, the secretion levels of IFN-γ were not different in these three groups (Figure 5B). We then tested the changes in IFN-γ secretion levels after 72 h in all experimental groups of PD1−CD8+ TILs, and the results showed the most obvious change in the αPD1-NPs-DAC group, which had significantly higher levels than the other groups (Figure 5C); in PD1−CD8+ TILs, IFN-γ secretion levels in the saline, empty NPs, free DAC, free nivolumab, free DAC + free nivolumab, αPD1-NPs, NPs-DAC, and αPD1-NPs-DAC groups showed no significant differences ($p > 0.05$) (Figure 5D).

In vivo investigations

Animal models were established as a saline group, a free DAC group, an NPs-DAC group, a free nivolumab group, an NPs-DAC+αPD1 group, and an αPD1-NPs-DAC group. Changes in tumor volumes were observed for 40 days after tumor inoculation, and survival curves were also plotted. As shown in Figure 6A, although all groups showed similar tumor sizes by the 40th day after tumor inoculation, the tumor volumes in the saline group were obviously higher than those in the free DAC and NPs-DAC groups. Moreover, the tumor volumes were gradually reduced in the free nivolumab group and NPs-DAC+αPD1 group, with the αPD1-NPs-DAC group showing the smallest tumor size. As shown in Figure 6B, the survival curve of the animal groups also indicated better survival rate in the αPD1-NPs-DAC group and NPs-DAC+αPD1 group. Meanwhile, the free nivolumab and NPs-DAC group showed better survival rates than the saline group, although lower than that of the NPs-DAC+αPD1 group. TUNEL assay of the implanted tumor also validated the growth of tumor in different animal groups (Figure 6C). Moreover, the toxicity indicated by the results of H&E staining of heart tissues (Figure 7A), kidney tissues (Figure 7B), and bowel tissues (Figure 7C) showed no difference between different groups.

DISCUSSION

Here, αPD1-NPs-DAC was produced for GC treatment using a novel nivolumab-conjugated nanoscale drug delivery vehicle. We confirmed that nivolumab-conjugated NPs effectively delivered

Table 2. Mean particle size and drug load efficiency of four kinds of nanoparticles

Nanoparticles	Diameter, nm[a]	Polydispersity[a]	Zeta Potential, mV[a]	DAC DLC, % DAC EE, %	Nivolumab Content, % w/w
PEG-PCL	164.2 ± 4.6	0.196 ± 0.061	−9.17 ± 1.37	–	–
DAC-PEG–PCL	181.8 ± 3.5	0.223 ± 0.07	−8.16 ± 1.82	8.11 ± 0.12 57.32 ± 2.3	–
αPD1-PEG-PCL	186.5 ± 5.3	0.179 ± 0.051	−9.14 ± 1.29		3.84 ± 0.23
αPD1-PEG-PCL-DAC	217.5 ± 6.7kuw	0.301 ± 0.045	−10.93 ± 0.73	8.21 ± 0.18 59.2 ± 3.2	3.62 ± 0.19

DLC, drug loading content; EE, encapsulation efficiency.
[a]The SD value is for the mean particle size obtained from three measurements.

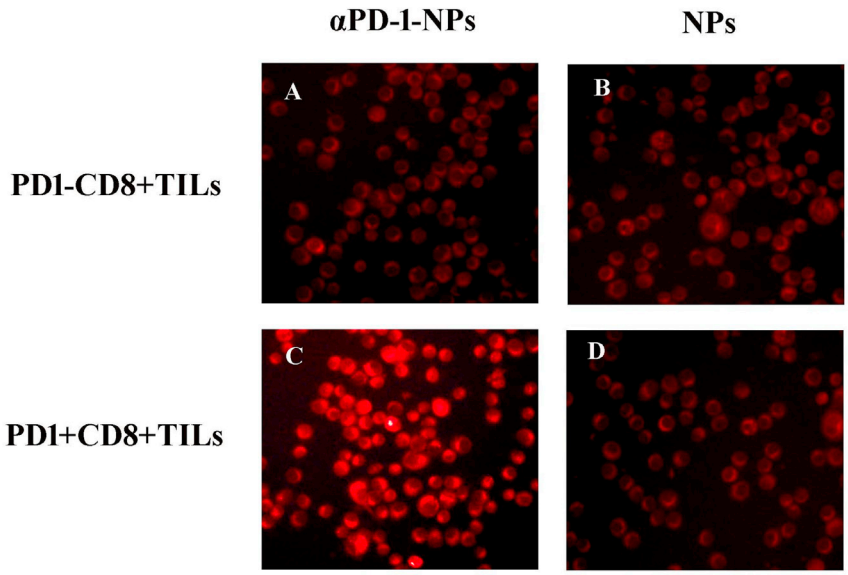

Figure 2. Fluorescent signal of TILs incubated with DID loaded NPs or αPD1-NPs

(A and B) PD1−CD8+ TILs incubated with DiD-loaded NPs (A) or αPD1-NPs (B). (C and D) PD1+CD8+ TILs incubated with DiD-loaded NPs (C) or αPD1-NPs (D). The fluorescent signal clearly deposited mostly at the periphery of the cells, with little fluorescent signal observed inside the nuclei. The fluorescence intensities of both TILs were similar. Scale bars, 50 μm (left) and 20 μm (right). PD1+CD8+ TILs, tumor-infiltrating PD1+CD8+ T cells.

DAC into PD1+CD8+ TILs. They significantly suppressed the growth of autologous tumor cells co-cultured with PD1+CD8+ TILs compared with other groups, upregulating IFN-γ. Notably, the delivery of DAC with nivolumab-conjugated NPs enhanced apoptosis in autologous tumor cells in comparison with either drug alone following a 72 h incubation. Combination treatment also elevated the secretion IFN-γ in PD1+CD8+ TILs, which functions as the most important anti-tumor cytokine secreted by cytotoxic T cells. Of note, these synergistic effects were not detected in PD1−CD8+ TILs, likely because there is no IFN-γ content elevation in this subtype of TILs after the administration of αPD1-NPs-DAC. Reinvigorating exhausted CD8+ T cells by PD1 blockade treatment is currently a highly promising frontier in cancer treatment. However, T cell rejuvenation might be transient.[15] Ghoneim et al.[16] demonstrated that the progressive *de novo* DNA methylation programming further repressing major effector cytokines such as IFN-γ is critical for PD1+CD8+ TIL exhaustion. It was also demonstrated that prolonged exhaustion-related epigenetic changes constitute an important cell-intrinsic barrier that limits antigen-specific CD8+ T cell rejuvenation during PD1 blockade treatment. These data reveal epigenetic changes in PD1+CD8+ TILs as a possible mechanism underpinning PD1 blockade's treatment failure.[17] Consistently in our experiments, we found that the IFN-γ methylation level of PD1+CD8+ TILs was significantly higher than that of PD1−CD8+ TILs (Table 4). Given this background, we have now extended our approach to combination therapy of ICI and DAC, a well-tolerated DNA hypomethylating drug to subtype TILs from individuals with GC.

An NP-based delivery system increases drug stability and delivery efficiency; NP-based delivery might occur through active or passive targeting.[18] Passive targeting is promoted by EPR or local application and delivery, which leads the loading drug traffic to the tumor microenvironment (TME) first. Active targeting involves the conjugation of various targeting groups to the surface of NPs, which anchor specific cells in the TME.[19] Antibodies, as ideal anti-tumor molecules, have been widely examined for five decades, with some successfully applied as immuno-targeting molecules.[20] We previously linked antibodies (e.g., trastuzumab) to NP surface for targeted delivery of anti-miR21.[21] We also effectively delivered DAC using PEG-PCL-based NPs targeting malignant cells, which increased DAC stability and induced 5-Fu cytotoxicity to GC cells via demethylation of TFAPE.[22] In this work, NPs of copolymers PEG-PCL linked to nivolumab for targeted delivery of DAC to the population of PD1+CD8+ TILs were produced (Figure 1B). The best formulation was next assessed for DAC delivery into PD1+CD8+ TILs. A nivolumab-to-PEG-PCL mass ratio of 1:1 resulted in efficient conjugation (Table 1). Free amino groups on NPs constituted linkers for the ligand in presence of EDAc. The NPs produced by double-emulsion solvent evaporation approximated 200 nm in size, with negative zeta potential values, promoting cell uptake by endocytosis[23] (Figure 1B; Table 2). This promoted DAC loading and inhibited its degeneration under 50% FBS (Figure 1C; Table 1), indicating similar mechanisms in the vessels and TME. Besides, we also found that the particle sizes of PEG-PCL NPs, αPD1-PEG-PCL-NPs, and αPD1-PEG-PCL-NPs-DAC were stable for more than 14 days (Figure 1D).

Non-specific interactions between nanocarriers and non-target cells limit treatment efficacy and cause deleterious effects. In comparison with PEG-PCL, including PD1 in the formulation significantly increased cell uptake in PD1+CD8+ TILs. Furthermore, we established the targeted uptake using PD1−CD8+ TILs as a control. We found that the fluorescence of DiD-loaded NPs in PD1−CD8+ TILs was almost as strong as that of PD1+CD8+ TILs (Figures 3A and 3B). Besides, the cellular uptake of DiD-NPs was similar in PD1+CD8+ TILs and PD1−CD8+ TILs (Figures 2B and 2D). The decreased uptake of DiD-TNPs in PD1−CD8+ TILs compared with PD1+CD8+ TILs further demonstrated αPD1-NP entry into TILs is controlled by nivolumab-mediated endocytosis (Figures 2C and 2D). The cellular effects of formulations with nivolumab linked to nanocarriers were increased by active entry into TILs producing PD1. Indeed, elevated cell uptake of αPD1-PEG-PCL NPs is important for optimal treatment efficiency.

Table 3. Integrated optical densities (IODs) of DiD-NPs and DiD-αPD1-NPs in PD1+CD8+ TILs and PD1–CD8+ TILs using ImageJ software

Variable (IOD)	NPs[a]	αPD1-NPs	p Value
PD1+CD8+ TILs	53,621 ± 424.3	95,171 ± 675.7	<0.001*
PD1−CD8+ TILs	41,223 ± 521.7	40,135 ± 591.2	>0.05
p value	>0.05	<0.001*	

[a]The SD value is for the mean IOD obtained from three measurements.

Demethylating agents not only reactivate the expression of genes contributing to drug resistance but also upregulate cytotoxic T cell effectors such as IFN-γ, which are suppressed in the tumor microenvironment by epigenetic modifications. Recent experimental approaches reported an immune-based mechanism of action of DNA methyltransferase inhibitors.[24] Therefore, a combination of new immunotherapeutic agents of the immune checkpoint inhibitor class and epigenetic modulators is considered a potential treatment tool in cancer therapy. For example, Peng et al.[25] showed that DAC upregulates tumor CXCL10, increasing effector T cells in the TME and improving response to αPDL1 treatment. Others have revealed that decitabine increases activated immune cell amounts in ovarian ascites and sensitizes tumors to α-CTLA4, a cytotoxic T lymphocyte-associated protein.[26] Epigenetic drugs upregulate a cytosolic sensing double-stranded RNA (dsRNA) antiviral pathway, inducing type I IFN synthesis and downstream pathways to upregulate IFN-induced genes such as immune cell-attracting chemokines and cytokines.[24] Stone et al. demonstrated that epigenetic drugs activate type I IFN signaling in mouse ovarian cancer to decrease immunosuppressive reactions as well as tumor burden.[27] Among these epigenetic agents, DAC is the most studied drug and is applied in current MDS therapy. However, it shows reduced efficacy in solid tumors which might be associated with pharmacokinetic and pharmacodynamic differences between solid and hematologic cancers.[28] DAC induces the reactivation of genes suppressed by abnormal DNA methylation and thus is a promising strategy for PD1 blockade T cell rejuvenation.[17] In agreement, DAC delivered into co-cultured PD1+CD8+ TILs and autologous tumor cells via PD1-NPs in the present work resulted in enhanced apoptosis compared with the drug alone. This increased effect was tightly associated with elevated IFN-γ secretion. The increased growth suppression might involve both NP packaging and drug co-delivery effects on co-cultured PD1+CD8+ TILs and autologous tumor cells, featuring IFN-γ hypermethylation.

Of note, significant synergistic effects of αPD1-NPs-DAC on PD1+CD8+ TILs were not observed until 72 h post-treatment. When applying DAC, it should be noted that epigenetic alterations by epigenetic agents generally require multiple cycles of replication.

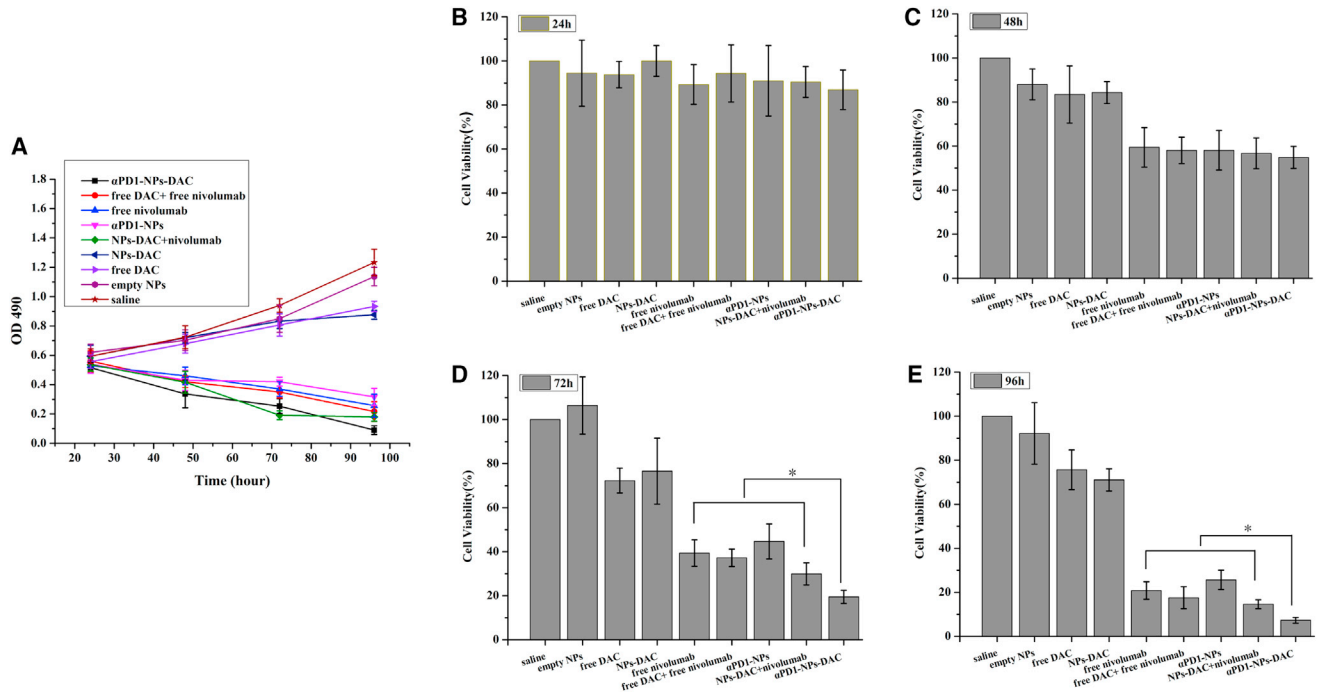

Figure 3. Comparison of the growth and cell viability of different cell groups

(A) Effects of free DAC (10 μmol/L), free nivolumab (1 μg/mL), empty NPs, free DAC + free nivolumab, blank αPD1-NPs (equal nivolumab concentration), NPs-DAC (equal DAC concentration), NPs-DAC+αPD1, and αPD1-TNPs-DAC on the growth of autologous tumor cells co-cultured with PD1+CD8+ TILs. Cell growth was determined using MTT assay every 24 h for 4 days. Saline was used as treatment control. (B–E) Cell viability was detected at 24 h (B), 48 h (C) 72 h (D), and 96 h (E) of treatment. *$p < 0.05$. DAC, 5-Aza-2′-deoxycytidine; NPs, nanoparticles; PD1+CD8+ TILs, tumor-infiltrating PD1+CD8+ T cells.

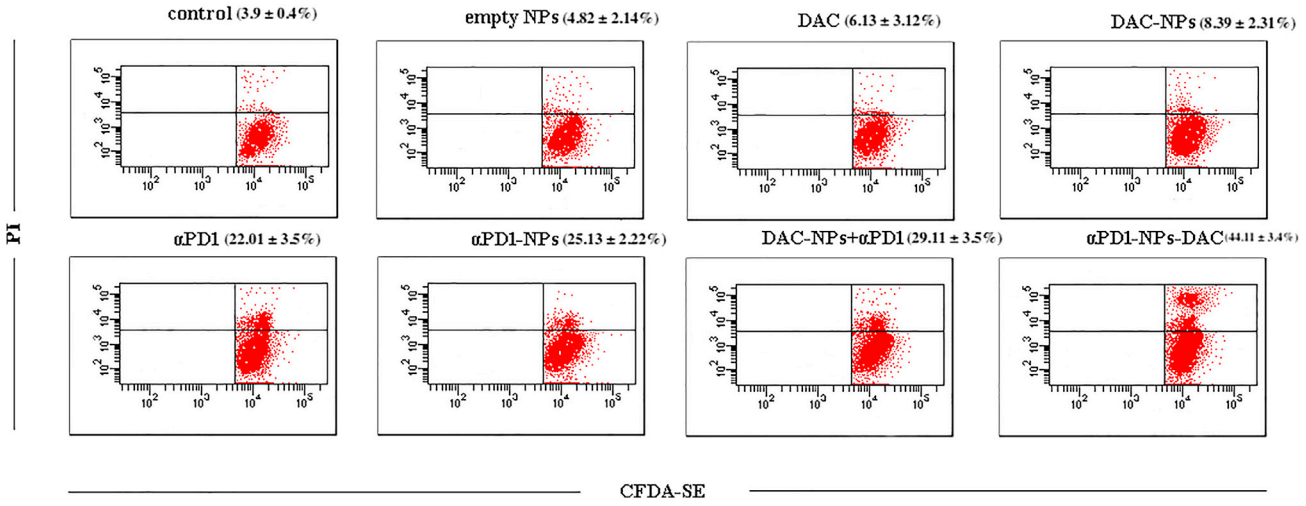

Figure 4. In vitro cytotoxicity of different cell groups

In vitro cytotoxicity of saline control, free DAC (10 μmol/L), free nivolumab (1 μg/mL), empty NPs, free DAC + free nivolumab, αPD1-NPs (equal nivolumab concentration), NPs-DAC (equal DAC concentration), NPs-DAC+αPD1, and αPD1-TNPs-DAC was evaluated in the co-culture system, in which CFDA-SE-labeled autologous tumor cells were cultured with PD1+CD8+ TILs. The rate of PI-positive and CFDA-SE-positive cells represented the death rate of tumor cells. Each value in the column diagram represents the mean ± SD (n = 3).

An important drawback of DAC is its easy degradation in aqueous solutions. Therefore, cell culture medium with DAC is commonly refreshed daily for 3 days before assessing the methylation status and/or expression alterations of genes.[21] Consequently, NPs promoting sustained DAC release might be advantageous, as prolonged release could enhance the synergistic effects of epigenetic treatment and immunotherapy. As shown above, DAC's retention curve (Figure 1D) revealed that encapsulated DAC remained stable for a time period up to 3-fold longer compared with free DAC in the aqueous environment at 37°C. Whereas residual free DAC amounts continuously decreased, NPs-DAC and αPD1-NPs-DAC amounts were first increased within the initial several hours and subsequently decreased slowly. This phenomenon may be explained by the observation that both types of nanoparticles showed a continuous release pattern with an initial burst of release, followed by sustained release. DAC from NPs was released significantly faster than it was degraded within 10 h of treatment; in the following time period, release from NPs started to level off before decreasing gradually and eventually becoming slower than drug degradation. Therefore, residual DAC amounts for both NPs first increase and then decrease to a certain time point. Accordingly, αPD1-NPs-DAC prolonged DNA demethylation of DAC on IFN-γ in PD1+CD8+ TILs co-cultured with autologous tumor cells, inducing a sustained elevation of IFN-γ secretion by PD1+CD8+ TILs (Figures 5A and 5C), which could partly explain the synergistic suppressive effects of autologous tumor cells by αPD1-NPs-DAC following 72 h treatment. Such upregulation was not found in the free DAC group. In addition, in PD1−CD8+ TILs co-cultured with autologous tumor cells (negative control), no significantly altered IFN-γ secretion was found following treatment with αPD1-NPs-DAC (Figures 5B and 5D). These findings corroborated previously reported data demonstrating that DAC administered with PD1 blockade enhances the rejuvenation of exhausted TILs, suggesting that targeting IFN-γ hypermethylation might be a potential tool for overcoming PD1 blockade resistance.[21] Therefore, this study confirmed that nivolumab-NP encapsulation could not only help stabilize DAC in culture, sustaining its demethylation effects, but also increase therapeutic efficiency in GC cells co-cultured with PD1+CD8+ TILs administered DAC.

Taken together, a potent *in vitro* T cell-targeting drug delivery system was designed. The targeted NP system delivering an epigenetic modifying agent could reverse PD1+CD8+ T cell exhaustion and ameliorate T cell responses as well as tumor control in the setting of immune checkpoint blockade as follows: (1) DAC delivery is specific and efficient, with improved DAC stability and cellular uptake thanks to PD1 and passive targeting approaches. (2) This strategy increases the targeting efficiency and immune checkpoint blockade biological functions of nivolumab. (3) The addition of an epigenetic agent enhances the reaction of cancer cells co-cultured with PD1+CD8+ TILs to immune checkpoint blockade drugs. This novel tool has fostered animal studies of tumor suppression. In a previous study, we performed real-time near-infrared fluorescence (NIRF) imaging to demonstrate antibody-linked NPs are superior to copolymeric NPs in drug delivery to the tumor microenvironment.[21] In addition, NIRF signals were significantly stronger in the tumor compared with other organs, demonstrating specific targeting of tumors according to NP distribution.[29] Similar studies by our group are ongoing for αPD1-NPs-DAC. The plasma half-life of DAC in the human body approximates 15–25 min, because of the extremely elevated activity of cytidine deaminase that inactivates this drug in the liver and spleen.[10] Theoretically, NPs should protect the loaded DAC from cytidine deaminase deamination through the EPR effect and antibody-mediated active

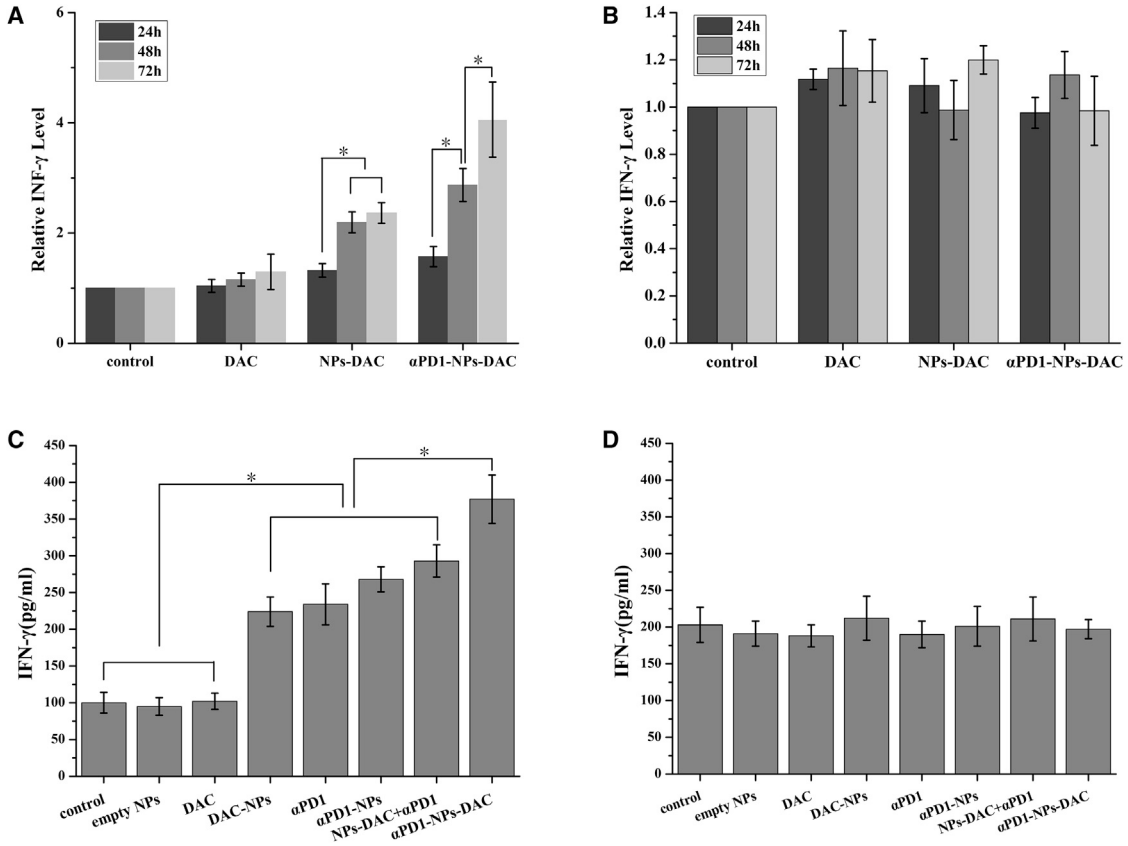

Figure 5. Autologous tumor cells were co-cultured with PD1+CD8+ TILs

(A and B) Supernatants were collected after different treatments (from left to right, saline control, DAC, NPs-DAC, and αPD1-NPs-DAC) at different times (24, 48, and 72 h) and measured for IFN-γ production using ELISA. (C and D) Supernatants were collected after treatment with saline, empty NPs, DAC, αPD1, αPD1-NPs, NPs-DACα+PD1, and αPD1-NPs-DAC at 72 h and measured for IFN-γ production using ELISA. Representative data from multiple gastric cancer donors (n = 12) are shown. DAC, 5-Aza-2′-deoxycytidine; NPs, nanoparticles; PD1+CD8+ TILs, tumor-infiltrating PD1+CD8+T cells.

targeting approach. Animal experiments are required to validate the present findings.

MATERIALS AND METHODS

Samples

Primary tumor tissues were collected from individuals with GC (n = 12) with surgically resectable tumors. Written informed consent was obtained from all participants before the initiation of the study, and the study was approved by the institutional ethics committee. Demographic and clinicopathological characteristics of all participants were collected and are presented in Table 5.

PEG-PCL copolymer synthesis

PEG-PCL copolymer synthesis was performed as reported in a previous study.[30] In brief, MePEG or PEG (50 g, 10 mmol) was added to ε-CL (1.15 g) and stannous octoate (0.05 g). The sealed tube containing the mixture was incubated at 130°C for 48 h. The resulting polymers dissolved in dichloromethane (DCM) underwent precipitation in large amounts of cold ethyl ether for removing monomers and oligomers. Finally, precipitate filtration was performed before drying under low pressure.

αPD1 mAb linking and ligand density on the surface of PEG-PCL copolymers

The αPD1 mAb conjugate was obtained as reported previously.[31] In brief, dry PEG-PCL NPs were reacted with αPD1 mAb in borate buffer in presence of EDAc and Sulfo-NHS overnight at ambient. The NPs were then prepared by centrifugation. The antibody amounts on the NPs were assessed by subtracting supernatant amounts (obtained using ELISA) from total concentrations.

Preparation of DAC-loaded NPs

Drug-loaded NPs were obtained as previously proposed.[29] In brief, DAC (0.25 mg/mL) was mixed with the copolymer (30 mg). The mixture was added slowly to 5% polyvinyl alcohol (PVA), followed by sonication to generate a water-in-oil-in-water (W/O/W) emulsion, which was added to aqueous 0.3% (v/v) PVA and stirred for 3 h. This was followed by filtration (1-μm-pore membranes; GE Whatman,

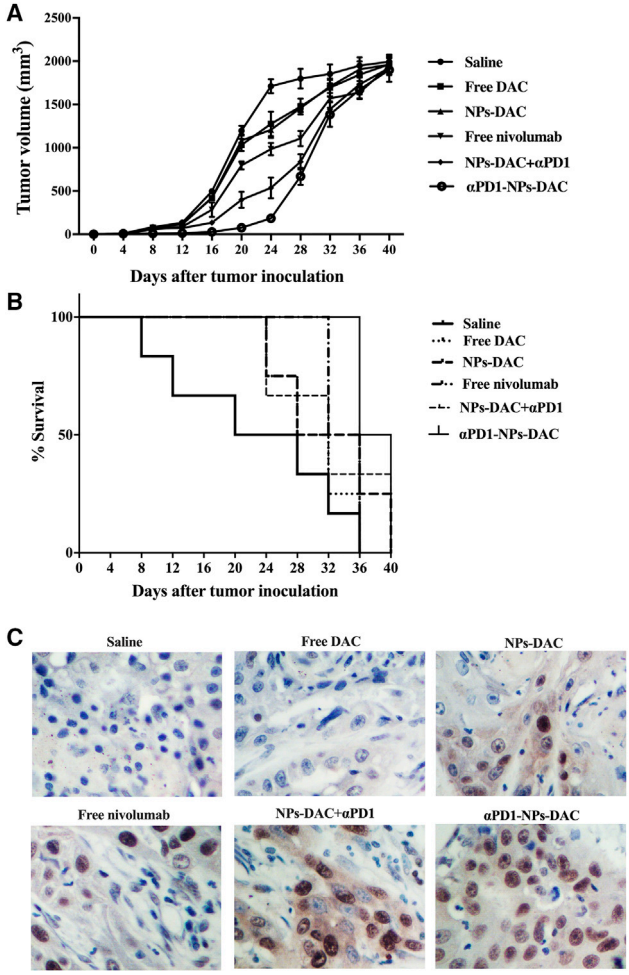

Figure 6. Animal models were established as a saline group, a free DAC group, an NPs-DAC group, a free nivolumab group, an NPs-DAC+αPD1 group, and an αPD1-NPs-DAC group

(A) Although all groups showed similar tumor sizes by the 40th day after tumor inoculation, the tumor volumes in the saline group were obviously higher than these in the free DAC and NPs-DAC groups. Moreover, the tumor volumes were gradually reduced in the free nivolumab group and NPs-DAC+αPD1 group, with the αPD1-NPs-DAC group showing the smallest tumor size. (B) Better survival rate in the αPD1-NPs-DAC group and NPs-DAC+αPD1 group was observed, and the free nivolumab and NPs-DAC group showed a better survival rate than the saline group, although lower than that of the NPs-DAC+αPD1 group. (C) TUNEL assay of the implanted tumor also validated the growth of tumor in different animal groups.

Xinhua, China). Pluronic F68 (40 mg/mL) was used for lyophilization of the NPs. NPs encapsulating DAC or combinations with DiD (Life Technologies) were prepared by the same techniques.

Surface chemistry of the NPs

The presence of αPD1 mAb on NPs surface was assessed using the XPS software. The NPs' surface was also examined for the specific binding energy (eV) of the constituents (eV = 0–1,000 eV, with pass energy at 80 eV under fixed transmission. Nitrogen was detected at 0.5 eV.

Physicochemical features of the NPs

NPs were examined for size, polydispersity, zeta potential, and morphological properties. Hydrodynamic size and polydispersity were assessed using dynamic light scattering (DLS) equipment (Brookhaven Instruments). Zeta potential was obtained using a ZetaPlus (Brookhaven Instruments). Specimens were stored at 37°C in PBS, with size monitoring for 16 days to determine stability. Morphological studies were carried out by transmission electron microscopy on a JEM-100S (JEOL) using routine methods after negative staining with phosphotungstic sodium (1% w/v).

Drug loading amounts and encapsulation efficiency

DAC degradation to N-β-D-2-deoxyribofuranosyl-3-guanylurea (DGU) in solution at 5°C is below 1% within 24 h.[7] Thus, lyophilized NPs were mixed with the solvent and stirred at 100 rpm for 12 h at 4°C. Drug loading content (DLC) and encapsulation efficiency were assessed using high performance liquid chromatography (HPLC) on an Agilent 1200 HPLC system equipped with a C18 reversed phase column (250 × 4.6 mm, 5 μM). DAC elution was performed with 0.01 M K_2HPO_4 buffer (pH 6.8). Samples (20 μL) were injected at 1.0 mL/min, with detection at 220 nm. DLC and EE were obtained as shown in Equations 1 and 2, respectively:

$$DLC\% = \frac{Weight\ of\ the\ drug\ found\ loaded}{Weight\ of\ the\ drug - loaded\ nanoparticles} \times 100\% \quad \text{(Equation 1)}$$

$$EE\% = \frac{Weight\ of\ the\ drug\ found\ loaded}{Weight\ of\ the\ drug\ input} \times 100\% \quad \text{(Equation 2)}$$

DAC decomposition assay for NPs-DAC in PBS and cell culture

After lyophilization, NPs (50 mg) underwent resuspension in 2 mL PBS (pH 7.4) and dialysis (12 kDa molecular weight cutoff membrane; Sigma-Aldrich) against PBS with shaking at 37°C for 72 h. At given times, 0.1 mL of the released solution was collected for HPLC assessment and replaced with the same amount of PBS. A DAC solution (about the same amount of encapsulated DAC) in PBS (pH 7.4) was run as a control in decomposition analysis. Because of DAC instability at 37°C in aqueous solutions, the residual DAC at various times for both NPs-DAC and αPD1-NPs-DAC with identical amounts of free DAC was used as control. The decomposition levels of encapsulated and free DAC were then assessed.

Cell isolation and DNA methylation assessment

TILs used in these experiments were isolated from individuals with GC, who underwent surgical removal of primary gastric tumors. The study had approval from the ethics committee of the First Affiliated Hospital of Lianyungang. Signed informed consent was provided by each participant. Following surgery, tumor samples were processed as reported in a previous study.[32] In brief, tissue mincing was followed by digestion with collagenase I (Sigma-Aldrich) and DNase in RPMI 1640 at 37°C. Next, the cells were passed through a cell strainer (70 μm) and submitted to PBS washing. TILs produce

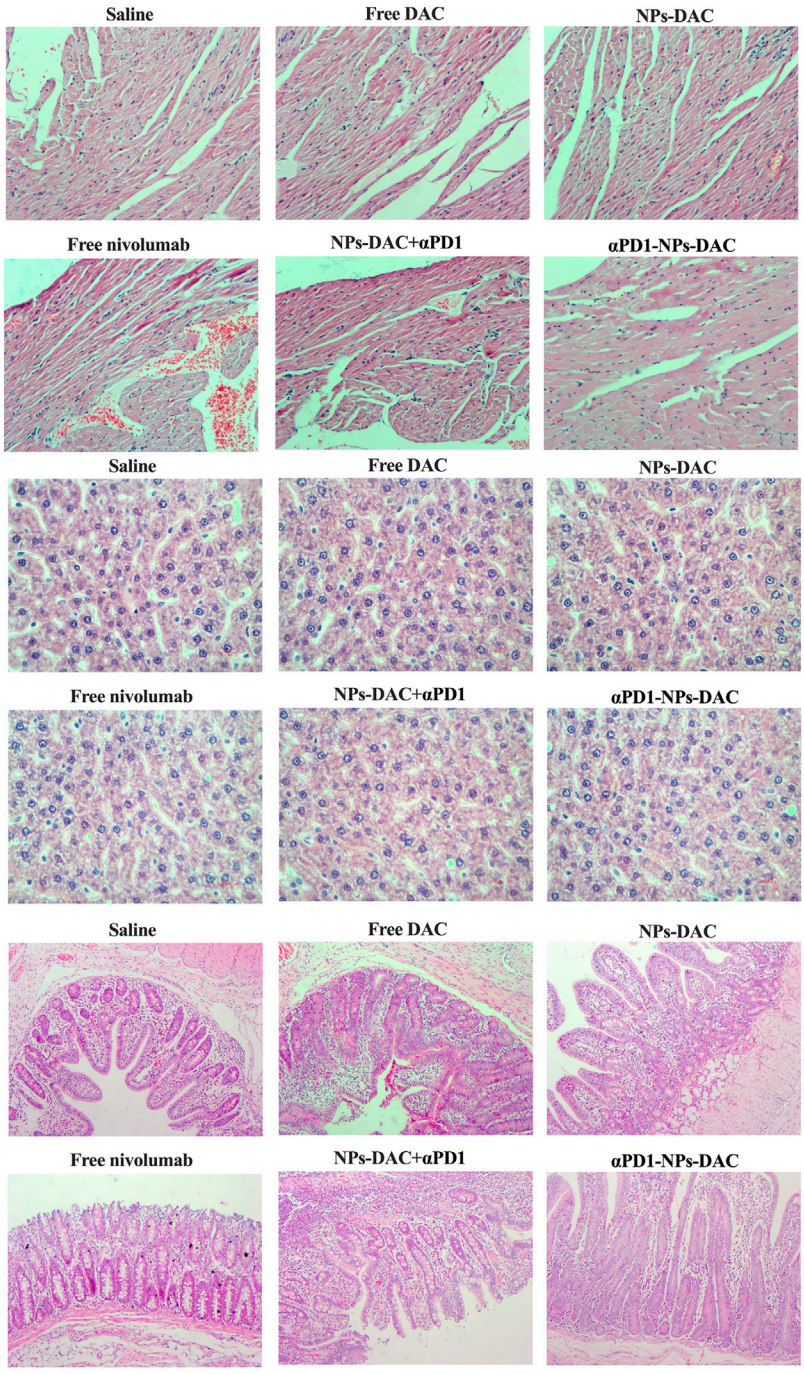

Figure 7. HE staining of tissues collected from different animal groups

(A–C) H&E staining of heart tissues (A), kidney tissues (B), and bowel tissues (C) showed no difference of toxicity among different groups. PEG-PCL NPs were linked to the αPD1 antibody nivolumab to yield αPD1-NPs for targeting TILs with PD1 overexpression. We found that the NPs increased DAC stability and improved IFN-γ secretion and the anti-tumor effect of ICB *in vitro*, suggesting that nivolumab-NPs are a potential tool for delivering epigenetic drugs in gastric cancer.

elevated amounts of immune inhibitory proteins (e.g., PD1).[33] CD8+PD1+ and CD8+PD1− cells were separated from TILs using flow cytometry on a FACS Influx. Genomic DNA samples from the sorted CD8+PD1+ and CD8+PD1− cells were obtained with the QIAamp DNA Mini Kit (Qiagen).[34] Primers for methylated IFN-γ encompassing CpGs in the second CpG island were designed using MethPrimer 2.0 (forward 5′-GTTATTTAGGTTGGAGTGTAGT GGC-3′ and reverse 5′-CCCAACACTTTAAAA AATTAAAACG-3′; probe, 5′-TGGGTTTAAGT TATTTTTTTGTTTAGTTT-3′). Amplification was carried out for 10 min at 95°C, followed by 50 cycles of 15 s (95°C), 30 s (60°C), and 10 s (72°C). Methylation of beta-actin was used for normalization. Data were expressed as methylation ratio (PMR), as a percentage. IFN-γ PMRs in PD1+CD8+ and PD1−CD8+ TILs were 96.7% and 15.3%, respectively (Table 4).

In vitro cellular uptake study

Particles were first incubated with DiD, a fluorescent molecule mimicking DAC. Sorted PD1+CD8+ and PD1−CD8+ TILs were cultured at various levels of DiD or 30 min at 37°C, followed by three to five PBS washes. An Olympus LX71 epifluorescence microscope was used for data analysis.

Cell viability assay

The cytotoxicity of NPs was examined using the MTT assay. Co-cultured cells (PD1+CD8+ or PD1−CD8+ TILs with autologous cancer cells) were seeded (5:1 ratio) in 96-well plates at 4,000 cells/well for a 24 h incubation. Then, saline, empty NPs, DAC (10 μmol/L, 2,228 μg/L), αPD1 (3 nmol/L, 145,000, 43.5 μg/L), αPD1-NPs (equal nivolumab levels), NPs-DAC (equal DAC levels), and αPD1-NPs-DAC (equal DAC and nivolumab concentrations) were added for 72 h. The culture medium was discarded after centrifugation, followed by careful rinsing with PBS (two or three times). Then, the culture medium containing MTT was added, and optical density at 490 nm was read daily for 4 days.

Mortality and cytokine level assessment in co-cultures

Autologous cancer cells were obtained as reported in a previous study.[32] Briefly, resected GC specimens underwent mincing and incubation with collagenase I (2 mg/mL) and DNase I (50 U/mL). This

Table 4. DNA methylation level of IFN-γ in PD1+CD8+ TILs and PD–CD8+ TILs

TILs	PD1+CD8+ TILs	PD−CD8+ TILs
PMR, %[a]	96.7 ± 4.8	15.3 ± 2.5

PMR, percentage of methylation ratio; TILs, tumor-infiltrating lymphocytes.
[a]The SD value is for the mean particle size obtained from three measurements.

was followed by filtration (cell strainer). Non-hematopoietic (CD45−) cells collected using flow cytometry constituted autologous cancer cells, which underwent labeling with CFDA-SE.[35] CFDA-SE-stained cells underwent resuspension to 1×10^5 cells/mL in RPMI 1640 and were used as target cells (T). Meanwhile, sorted PD1+CD8+ and PD1−CD8+ TIL suspensions underwent adjustment to 4×10^6 cells/mL in RPMI 1640 and were used as effector cells (E). Co-cultures were performed in 12-well plates (1 mL) at a 5:1 E/T ratio. Target cells were also incubated without effector cells to assess spontaneous cell death. Following 4 h incubation, co-cultured cells underwent further treatment with saline, empty NPs, DAC, αPD1, αPD1-NPs, NPs-DAC, and αPD1-NPs-DAC for 72 h. After incubation, effector cells and autologous tumor cells underwent staining with propidium iodide (PI). Autologous tumor cell death (CFDA-SE+/PI+ cell ratio) was examined using flow cytometry on a BD FACS Atira II as previously reported.[36] To quantify cytokine release by T cells, culture supernatants were assessed for IFN-γ amounts by ELISA with a kit from R&D Systems as directed by the manufacturer.

Animal experiments

In this study, to establish the animal models for *in vivo* analysis, we used a total of 48 inbred specific pathogen-free (SPF) grade strain 615 mice (H-2Kk) aged 6–8 weeks and weighing 20–25 g. Furthermore, we used gastric cancer cells isolated from participant gastric tumor to inoculated the mice in the right armpit after different treatment, as described previously. The mice were randomly allocated into six groups with 8 mice in each group: the saline group, the free DAC group, the NPs-DAC group, the free nivolumab group, the NPs-DAC+αPD1 group, and the αPD1-NPs-DAC group. The gastric tumors were measured every 4 days after inoculation for 40 days. Relative tumor volumes were calculated with the absolute tumor volume in reference to the average tumor volume of the group on day 1. Meanwhile, the mice were monitored three times each week to check the conditions of morbidity and mortality associated with tumor growth and metastasis. Survival curves were plotted for each animal group. By the 40th day after tumor inoculation, the mice were sacrificed, and heart, kidney, and bowel samples were collected for subsequent toxicity analysis using H&E staining. This study was approved by the institutional ethics committee.

Table 5. Characteristics of individuals with gastric cancer

Characteristic	Number of Affected Individuals
Age	
>60 y	8
<60 y	4
Gender	
Female	7
Male	5
Tumor stage	
I	2
II	5
III	5

Statistical analysis

Data are expressed as mean ± SD and were compared using the Mann-Whitney U test. A p value < 0.05 indicated statistical significance.

ACKNOWLEDGMENTS

This work was supported by the National Natural Science Foundation of China (81802347), the Jiangsu Provincial Social Development Project Foundation (BE2019693), and a clinical research project of Wu Jieping Foundation (320.6750.19058).

AUTHOR CONTRIBUTIONS

N.H. and F.W. planed the study. W.L., Y.H., and Z.Z. performed the literature search. N.H., W.L., Y.H., and Z.Z. performed the experiments. J.Z., X.W., K.Z., and F.W. analyzed and visualized the data. N.H., W.L., and Y.H. wrote the manuscript. F.W. edited the manuscript. All other co-authors approved the final manuscript.

DECLARATION OF INTERESTS

The authors declare no competing interests.

REFERENCES

1. Sung, H., Ferlay, J., Siegel, R.L., Laversanne, M., Soerjomataram, I., Jemal, A., and Bray, F. (2021). Global cancer statistics 2020: GLOBOCAN estimates of incidence and mortality worldwide for 36 cancers in 185 countries. Cancer J. Clin. *71*, 209–249.
2. Jakus, A.E. (2016). Cancer immunotherapy: dual action of targeted T cells. Nature *538*, 8–9.
3. Sharma, P., and Allison, J.P. (2015). Immune checkpoint targeting in cancer therapy: toward combination strategies with curative potential. Cell *161*, 205–214.
4. Wherry, E.J. (2011). T cell exhaustion. Nat. Immunol. *12*, 492–499. https://doi.org/10.1038/ni.2035.
5. Gonda, T.A., Fang, J., Salas, M., Do, C., Hsu, E., Zhukovskaya, A., Siegel, A., Takahashi, R., Lopez-Bujanda, Z.A., Drake, C.G., et al. (2020). A DNA hypomethylating drug alters the tumor microenvironment and improves the effectiveness of immune checkpoint inhibitors in a mouse model of pancreatic cancer. Cancer Res. *80*, 4754–4767.
6. Brown, R., and Plumb, J.A. (2004). Demethylation of DNA by decitabine in cancer chemotherapy. Expert Rev. Anticancer Ther. *4*, 501–510.
7. Jabbour, E., Issa, J.P., Garcia-Manero, G., and Kantarjian, H. (2008). Evolution of decitabine development: accomplishments, ongoing investigations, and future strategies. Cancer *112*, 2341–2351.
8. Covey, J.M., and Zaharko, D.S. (1984). Effects of dose and duration of exposure on 5-aza-2′-deoxycytidine cytotoxicity for L1210 leukemia in vitro. Cancer Treat Rep. *68*, 1475–1481.

9. Karahoca, M., and Momparler, R.L. (2013). Pharmacokinetic and pharmacodynamic analysis of 5-aza-2′-deoxycytidine (decitabine) in the design of its dose-schedule for cancer therapy. Clin. Epigenetics *5*, 3.

10. Chabot, G.G., Bouchard, J., and Momparler, R.L. (1983). Kinetics of deamination of 5-aza-2′-deoxycytidine and cytosine arabinoside by human liver cytidine deaminase and its inhibition by 3-deazauridine, thymidine or uracil arabinoside. Biochem. Pharmacol. *32*, 1327–1328.

11. Wang, C., Thudium, K.B., Han, M., Wang, X.T., Huang, H., Feingersh, D., Garcia, C., Wu, Y., Kuhne, M., Srinivasan, M., et al. (2014). In vitro characterization of the anti-PD-1 antibody nivolumab, BMS-936558, and in vivo toxicology in non-human primates. Cancer Immunol. Res. *2*, 846–856.

12. Kang, Y.K., Boku, N., Satoh, T., Ryu, M.H., Chao, Y., Kato, K., Chung, H.C., Chen, J.S., Muro, K., Kang, W.K., et al. (2017). Nivolumab in patients with advanced gastric or gastro-oesophageal junction cancer refractory to, or intolerant of, at least two previous chemotherapy regimens (ONO-4538-12, ATTRACTION-2): a randomised, double-blind, placebo-controlled, phase 3 trial. Lancet *390*, 2461–2471.

13. Schmid, D., Park, C.G., Hartl, C.A., Subedi, N., Cartwright, A.N., Puerto, R.B., Zheng, Y., Maiarana, J., Freeman, G.J., Wucherpfennig, K.W., et al. (2017). T cell-targeting nanoparticles focus delivery of immunotherapy to improve antitumor immunity. Nat. Commun. *8*, 1747.

14. Hu, N., Yin, J.F., Ji, Z., Hong, Y., Wu, P., Bian, B., Song, Z., Li, R., Liu, Q., and Wu, F. (2017). Strengthening gastric cancer therapy by trastuzumab-conjugated nanoparticles with simultaneous encapsulation of anti-MiR-21 and 5-fluorouridine. Cell Physiol. Biochem. *44*, 2158–2173.

15. Ribas, A., Hamid, O., Daud, A., Hodi, F.S., Wolchok, J.D., Kefford, R., Joshua, A.M., Patnaik, A., Hwu, W.J., Weber, J.S., et al. (2016). Association of pembrolizumab with tumor response and survival among patients with advanced melanoma. JAMA *315*, 1600–1609.

16. Ghoneim, H.E., Fan, Y., Moustaki, A., Abdelsamed, H.A., Dash, P., Dogra, P., Carter, R., Awad, W., Neale, G., Thomas, P.G., and Youngblood, B. (2017). De Novo Epigenetic Programs Inhibit PD-1 Blockade-Mediated T Cell Rejuvenation. Cell *170*, 142–157.

17. Youngblood, B. (2017). De novo epigenetic programs inhibit PD-1 blockade-mediated t cell rejuvenation. Cell *170*, 142–157.e119.

18. Das, M., Mohanty, C., and Sahoo, S.K. (2009). Ligand-based targeted therapy for cancer tissue. Expert Opin. Drug Deliv. *6*, 285–304.

19. Maeda, H., Wu, J., Sawa, T., Matsumura, Y., and Hori, K. (2000). Tumor vascular permeability and the EPR effect in macromolecular therapeutics: a review. J. Control Release *65*, 271–284. https://doi.org/10.1016/s0168-3659(99)00248-5.

20. Cirstoiu-Hapca, A., Buchegger, F., Lange, N., Bossy, L., Gurny, R., and Delie, F. (2010). Benefit of anti-HER2-coated paclitaxel-loaded immuno-nanoparticles in the treatment of disseminated ovarian cancer: therapeutic efficacy and biodistribution in mice. J. Control Release *144*, 324–331.

21. Liu, Q., Li, R.T., Qian, H.Q., Yang, M., Zhu, Z.S., Wu, W., Qian, X.P., Yu, L.X., Jang, X.Q., and Liu, B.R. (2012). Gelatinase-stimuli strategy enhances the tumor delivery and therapeutic efficacy of docetaxel-loaded poly(ethylene glycol)-poly(varepsilon-caprolactone) nanoparticles. Int. J. Nanomedicine *7*, 281–295.

22. Wu, F.L., Li, R.T., Yang, M., Yue, G.F., Wang, H.Y., Liu, Q., Cui, F.B., Wu, P.Y., Ding, H., Yu, L.X., et al. (2015). Gelatinases-stimuli nanoparticles encapsulating 5-fluorouridine and 5-aza-2′-deoxycytidine enhance the sensitivity of gastric cancer cells to chemical therapeutics. Cancer Lett. *363*, 7–16.

23. Iyer, A.K., Khaled, G., Fang, J., and Maeda, H. (2006). Exploiting the enhanced permeability and retention effect for tumor targeting. Drug Discov. Today *11*, 812–818.

24. Chiappinelli, K.B., Strissel, P.L., Desrichard, A., Li, H., Henke, C., Akman, B., Hein, A., Rote, N.S., Cope, L.M., Snyder, A., et al. (2015). Inhibiting DNA methylation causes an interferon response in cancer via dsRNA including endogenous retroviruses. Cell *162*, 974–986.

25. Peng, D., Kryczek, I., Nagarsheth, N., Zhao, L., Wei, S., Wang, W., Sun, Y., Zhao, E., Vatan, L., Szeliga, W., et al. (2015). Epigenetic silencing of TH1-type chemokines shapes tumour immunity and immunotherapy. Nature *527*, 249–253.

26. Roulois, D., Loo Yau, H., Singhania, R., Wang, Y., Danesh, A., Shen, S.Y., Han, H., Liang, G., Jones, P.A., Pugh, T.J., et al. (2015). DNA-demethylating agents target colorectal cancer cells by inducing viral mimicry by endogenous transcripts. Cell *162*, 961–973.

27. Stone, M.L., Chiappinelli, K.B., Li, H., Murphy, L.M., Travers, M.E., Topper, M.J., Mathios, D., Lim, M., Shih, I.M., Wang, T.L., et al. (2017). Epigenetic therapy activates type I interferon signaling in murine ovarian cancer to reduce immunosuppression and tumor burden. Proc. Natl. Acad. Sci. U S A *114*, E10981–E10990.

28. Strathdee, G., MacKean, M.J., Illand, M., and Brown, R. (1999). A role for methylation of the hMLH1 promoter in loss of hMLH1 expression and drug resistance in ovarian cancer. Oncogene *18*, 2335–2341.

29. Liu, Q., Li, R.T., Qian, H.Q., Wei, J., Xie, L., Shen, J., Yang, M., Qian, X.P., Yu, L.X., Jiang, X.Q., et al. (2013). Targeted delivery of miR-200c/DOC to inhibit cancer stem cells and cancer cells by the gelatinases-stimuli nanoparticles. Biomaterials *34*, 7191–7203.

30. Li, R., Li, X., Xie, L., Ding, D., Hu, Y., Qian, X., Yu, L., Ding, Y., Jiang, X., and Liu, B. (2009). Preparation and evaluation of PEG-PCL nanoparticles for local tetradrine delivery. Int. J. Pharm. *379*, 158–166. https://doi.org/10.1016/j.ijpharm.2009.06.007.

31. Liu, Y., Li, K., Liu, B., and Feng, S.-S. (2010). A strategy for precision engineering of nanoparticles of biodegradable copolymers for quantitative control of targeted drug delivery. Biomaterials *31*, 9145–9155.

32. Thommen, D.S., Koelzer, V.H., Herzig, P., Roller, A., Trefny, M., Dimeloe, S., Kiialainen, A., Hanhart, J., Schill, C., Hess, C., et al. (2018). A transcriptionally and functionally distinct PD-1(+) CD8(+) T cell pool with predictive potential in non-small-cell lung cancer treated with PD-1 blockade. Nat. Med. *24*, 994–1004.

33. Pardoll, D.M. (2012). The blockade of immune checkpoints in cancer immunotherapy. Nat. Rev. Cancer *12*, 252–264.

34. Ooki, A., Yamashita, K., Kikuchi, S., Sakuramoto, S., Katada, N., Kokubo, K., Kobayashi, H., Kim, M.S., Sidransky, D., and Watanabe, M. (2010). Potential utility of HOP homeobox gene promoter methylation as a marker of tumor aggressiveness in gastric cancer. Oncogene *29*, 3263–3275.

35. Wang, X.Q., Duan, X.M., Liu, L.H., Fang, Y.Q., and Tan, Y. (2005). Carboxyfluorescein diacetate succinimidyl ester fluorescent dye for cell labeling. Acta Biochim. Biophys. Sin (Shanghai) *37*, 379–385.

36. Roy, A., Chandra, S., Mamilapally, S., Upadhyay, P., and Bhaskar, S. (2012). Anticancer and immunostimulatory activity by conjugate of paclitaxel and non-toxic derivative of LPS for combined chemo-immunotherapy. Pharm. Res. *29*, 2294–2309.